

# KIFC1 is essential for normal spermatogenesis and its depletion results in early germ cell apoptosis in the Kuruma shrimp, *Penaeus (Marsupenaeus) japonicus*

Shuang-Li Hao<sup>1</sup>, Wan-Xi Yang<sup>1</sup>

<sup>1</sup>The Sperm Laboratory, College of Life Sciences, Zhejiang University, Hangzhou 310058, China

**Correspondence to:** Wan-Xi Yang; email: [wxyang@spermlab.org](mailto:wxyang@spermlab.org)

**Keywords:** spermatogenesis, apoptosis, KIFC1, acrosome formation, *Penaeus (Marsupenaeus) japonicus*

**Received:** July 1, 2019

**Accepted:** December 2, 2019

**Published:** December 29, 2019

**Copyright:** Hao et al. This is an open-access article distributed under the terms of the Creative Commons Attribution License (CC BY 3.0), which permits unrestricted use, distribution, and reproduction in any medium, provided the original author and source are credited.

## ABSTRACT

In order to explore the dynamic mechanisms during spermatogenesis of the penaeid prawns, the full length of *kifc1* was cloned from testis cDNA of *Penaeus japonicus* through RACE. Both semi-quantitative RT-PCR and Western blot results indicated that KIFC1 was extensively expressed in different tissue of *P. japonicus*. Compared with other tissue, the highest expression of KIFC1 occurred in the testis. According to the immunofluorescence results, the KIFC1 protein was detected at each stage of whole process of spermatogenesis. In the spermatogonial phase, KIFC1 mainly dispersed in cytoplasm and co-localized with microtubules, while abundant KIFC1 signal was detected in the nucleus of spermatocytes. At the early stage of spermatids, KIFC1 was transported from the nucleus into the cytoplasm, and it assisted microtubule assembly onto one side of the nucleus. Finally, in mature sperm, it was weakly expressed in the acrosome. This implies that KIFC1 may participate in the mitosis of spermatogonia, meiosis of spermatocyte, and acrosome formation during spermiogenesis; it may also play functions in acrosome maintaining in mature sperm. In addition, the results of KIFC1 knockdown by dsRNA injection *in vivo* reveal that decreased KIFC1 expression may induce aberrant microtubule assembly, and it leads to spermatogonia and spermatocyte apoptosis.

## INTRODUCTION

Mature and fertile sperm produced by spermatogenesis is the prerequisite for continuation of all gamogenetic species. Spermatogenesis is a complex and highly-ordered process that involves renewal and differentiation of spermatogonia stem cell, mitosis of spermatogonia, meiosis of spermatocyte, and the final dramatic morphological and cellular changes of spermiogenesis [1, 2]. For mammals, three prominent biological events occur during spermiogenesis, i.e., acrosome biogenesis, nucleus reshaping and tail formation. Finally, the swimming mature spermatozoa are produced [3]. However, spermatozoa of decapod crustaceans belong to non-flagella type and are immotile [4, 5]. The most notable morphological transformations during spermiogenesis in the testis are the formation of the special acro-

somal complex, reshaping and decondensation of the nucleus [6–8]. The acrosome originates from small preacrosomal vesicles. The small preacrosomal vesicles are formed from endoplasmic reticula which coalesce into a large acrosomal vesicle and gradually adhere to the nucleus [9–12]. Meanwhile, the nuclei of sperm become more and more decondensed during this process [9]. The final spermatid in the testis is not fully developed and mature spermatozoa. When the spermatogenesis process in the testis is finished, sperm are transferred into the vas deferens and then are enwrapped in the spermatophores [13]. This is not only a spermatozoa transport process, but also a post-testicular sperm maturation process, called post-spermiogenesis [14].

Increasing studies suggest that the network of cytoskeleton and molecular motors is essential for the

complicated dynamic spermatogenesis process [15, 16]. Microtubule is one of the major cytoskeletal components, which has a direct role in spermiogenesis in the form of manchette in mammal [17]. Although no manchette is reported by now in decapod crustaceans, microtubule bundles were observed [7]. Numerous papers have proven that cytoskeletal motors (kinesin, myosin and dynein) play essential roles during spermatogenesis such as the mitotic proliferation of spermatogonia [18–20], meiotic process of spermatocyte [21, 22], and spermiogenesis [17, 23]. Kinesin, a kind of microtubule-based motor protein, is also vital for different processes including microtubule organization [24] and vesicle transport [25]. The abnormal expression of kinesin motors results in spermatogenesis abnormalities and even male infertility in various species. KIF3A motor protein is one of the kinesin II subunit, which acts as a key regulator of spermatogenesis. Depletion of KIF3A leads to serious damage in the formation of sperm tail and at the same time, it also affects the organization of manchette and the shaping of sperm head [23]. Another kinesin family member, KIF18A, which belongs to the kinesin-8 family, widely expresses in proliferative tissues and is an important regulator of chromosome alignment during mitosis [26]. Loss of KIF18A function in mouse germ cell results in chromosome alignment defects and undergoes mitotic arrest and apoptosis [22].

KIFC1 is a member of the kinesin-14 family, which moves along the microtubules from the plus end to the minus end. It has been identified in various species and has a critical function in vesicular transport [17, 27], Golgi apparatus positioning and structural integrity [28], microtubule organization [29], spindle assembly and chromosome segregation [30]. In addition, KIFC1 is reported with a critical role in centrosome clustering in various cancer cells such as hepatocellular carcinoma and it has been suggested as a potential prognostic biomarker and therapeutic target for cancer treatment [31]. Interestingly, KIFC1 is closely related to maintaining of the normal spermatogenesis of Mammalia, Reptile, Amphibia, Crustacea, Cephalopoda, and Sipunculida [17, 32–35].

The Kuruma shrimp *P. japonicus*, belongs to family Penaeidae, Crustacea [36]. It is one of the model animals for studying the non-flagella spermatogenesis in decapod crustacea. Up to date, the kinetics mechanism of spermatogenesis in *P. japonicus* remains unknown. The purpose of our research is to investigate how kinesin motors play function during penaeid spermatogenesis. Therefore, we cloned the full length cDNA of *kifc1* gene of *P. japonicus* and explored its function in penaeid prawn for the first time. The expression pattern during spermatogenesis and the

result of KIFC1 knockdown by RNAi revealed KIFC1 may participate in mitosis and meiosis regulation, acrosome formation during spermatogenesis. The depletion of KIFC1 results in apoptosis of spermatogonia and spermatocytes.

## RESULTS

### The main features of *P. japonicus kifc1*

The full-length *kifc1* of *P. japonicus* is 2650 bp (GenBank accession number: MN072915). It contains 136 bp 5' untranslated region (UTR), 2217 bp open reading frame (ORF), and 297 bp 3' UTR. It encodes 738 amino acids and the predicted molecular weight is 81.10 kDa (Figure 1). The isoelectric point of this protein predicted by ExPASy-ProtParam tool is 9.47 (<https://web.expasy.org/protparam/>).

The secondary structure prediction of *P. japonicus* KIFC1 showed three primary domains. A divergent tail at the amino terminal is from 1 to 192 amino acids, a coiled stalk begins from 193 to 377 amino acids, and a head at the carboxyl terminal is composed of the 378–738 amino acids, which contains the conserved motor domain and “walks” along the microtubule (Figure 2A). Additionally, we predicted the putative tertiary structure of KIFC1 protein, in which all three domains' 3-D structures were observed clearly (Figure 2B–2E).

We aligned KIFC1 of *P. japonicus* with its homologues of other species and found it has 66.1%, 57.7%, 35.5%, 36.1%, 35.8%, 36.6%, 35.5% and 33.1% identity with its homologues in *Eriocheir sinensis*, *Macrobrachium nipponensis*, *Danio rerio*, *Bos taurus*, *Homo sapiens*, *Mus musculus*, *Gallus gallus*, and *Alligator sinensis*, respectively. The alignment result also showed a more conservative head region in KIFC1 when compared with the stalk and tail (Figure 3). In addition, there are three ATP binding sites (LAGSE, SSRSH and AYGQTGSGKT), a microtubule binding site (YNETIRDLL) and a KIFC conserved domain (ELKGNIRVFCRVRP) in the head region of *P. japonicus* KIFC1 (Figure 3). The phylogenetic analysis revealed the putative KIFC1 of *P. japonicus* constitutes a sister clade with its homologues of *Procambarus clarkii*, and also suggested it has a closest genetic relationship with *P. clarkii* among the examined species in this study (Figure 4).

### KIFC1 is highly expressed in reproductive system of *P. japonicus*

The expression of *kifc1* mRNA in different tissues of *P. japonicus* was determined using semi-quantitative RT-PCR. A 384 bp fragment of *kifc1* cDNA and a 179 bp

```

          acatggggagagcgttccctcccaagaaccgagttcaagctag
tsagttgggaattgtgttgacatttttggagatttcgagaaagaagaatccgactggtcttggagaaggccaag
atg tca aaa cta cct aca cct tcc agt cgc att aag tgc ccc gag ccc aca cgc ttg cgg
M S K L P T P S S R I K C P Q P T R L R
acc cca ggc tca gcc atg aag agc gag gcc agt ggc gca ctg cca gga tca cct gag
T P G S A M K R Q A S G A E L P G S P E
aag aag aca agc ctc agt gct tcc tcc att ggc tca aca gat tca gaa gat tet gtc cct
K K T R L S A S S I G S T D S E D S V P
gac atg cct cca cca gca cgt cgt ggc ctg act cgt caa cct aca gct cca gca ggg aaa
D M P P A R R G L T R Q P T A P A G K
cta aga cgg tet gtc tcc atg gcc agc tta ccc gfg agt ggt ctg agc gaa cgg aat ggt
L R R S V S M A S L P V S G L R E R N G
tcc aaa aca aac ctg gct cgt tcc aag ata ggg gca tca act cta aac ctc aca ggc agc
S K T N L A R S K I G A S T L N L T G R
gct tet aat aca cct gca aca gca gct aga aca tta gct ggc aaa gca cca get aga
A S N I T P A T A A R T L A G K A P A R
aga ccc ggc acc aac aac ccc aac gag gtc aac tet cgc agt gca gca gtc aca aag tcc
R P G T N I T N Q V N S R S A A V T K S
acc ggc act ggt ttg tca aat tca tet gfg gga gcc acc aag ccg ggt gga gat aca ggt
T G T G L S K S S V G G T K P G G D T G
agc aaa gga aag agc aaa agc ccg cca tgg gac etc aaa gga cgc ctg gag gat atg gaa
S K G C S K R P P W D L K G R L Q D M E
acc ctg gfg aag agc tgc gca gaa gaa cgc gag aac ttg atg gag aag ttc atg gac tac
T L V K S S A E R E N L M Q K F M D Y
gac ctg cgc att gag agc ctg gag cta gag aag agc agc etc aac gag aac ctg gag aag
D L R I E S L E L E K R S L N Q N L E K
acc gag agt gfg tet cag gcc acc gag gcc gag gtc gat cgc ctg agt acc aac cta aga
T Q S V S Q A T Q G E V D R L S T N L R
aat gag caa gat ggg aga agt gca gac aag agc aga tac gaa agt aca att gag gac cta
N E Q D G R S A D K R R Y E S T I Q D L
gaa ttc aat aaa gcc aca ctt gaa cgc gag ata aaa acc ttg gag tca gaa ctt tet gcc
E F N K A T L E R Q I K T L E S E L S A
aga caa gat gaa gct gca ggg ctg aag tgc aca gtc tct cat cta acg agt get cat gcg
R Q D E L A G L K S T V S H L T S A H A
ggc att gaa get cag ctg tca aca aag ata atg ctc gat gac cga aac aag aga gtc
G I E A Q L S S T K I M L D D R N K R V
tet gag etc gag tca cag gta gcc acc gag aca gac acc att gaa gac atg gag aaa aag
S E L E S Q V A T Q K D T I E D M E K K
ttg cgt gac gga gaa aat att agc cgg aag ctc cac aat acc gtc ctg gaa ctg aag ggt
L R D G E N I R R K L H N T V L E L K G

```

```

aat atc cgt gfg ttt tgc cga gfg aga ccc ctg ctt ggg gaa gag atc aag ggc aat gga
N I R V F C R V R P L L G E E I K G N G
gac agc gat gtc att cat cac atc agc ttt gtt gat gag aag acc ctt gaa ctg tgc aag
D S D V I H H I S F V D E K T L E L C K
gga gga gat ccc aac agc agc aca atg tgc ggc ctc aag ggc gga gga ggt gga gcc atc
G G D P N S S T M S G L K G R G G G A I
gag ttc aat tac gac cgg gtt ttc aac ccc acc agc tet cag gcc gag gfg ttt gag gag
E F N Y D R V F N P T S S Q A E V F E E
atc tgc cag ctg gcc cag tgc gcc etc gat ggc tac aac gtc tgc gtc ttt gcc tac ggc
I S Q L A Q S A L D G Y N V C V F A Y G
cag acg ggt tet ggg aag acc ttc acc atg gag gga atc cac ggc gag gag acg ctg gag
Q T G S G K T F T M E G I H G D E T L E
ggg atg atc cct cgc acc gtc aag cac atc ttc aag tcc atg aag gat ctt gaa gac aag
G M I P R T V K H I F K S M K D L E D K
ggc tgg aga tac aag gta gag gca agc ttt ttg gaa atc tac aat gaa acc ate aga gac
G W R Y K V E A S F L E I Y N E T I R D
ctg ctc gcc aec ccc aag gag tcc aag aat ctt acc tac gac gtc aag ctt gtc gac agc
L L A T P K E S K N L T Y D V K L V D S
aag aaa aac gat acc ttt gtc acc aat ctg aag gfg gtc gaa gta acc gaa agc cgt
K K N D T F V T N L K V V E V A N E S R
ggt cat cac ctc ctg acg ctt gcc cag caa cag aga gcc gtt gct gac acc aac atg aac
V H H L L T L A Q Q R A V A T N M N
gag agc tcc tcc cgg tcc cac tgc gtc ttc cgg etc aaa cta ggc cac aat agt aaa
E R S S R S H S V F R L K L T G H N S K
aca ctg gag tgt tgt gaa ggt aac ttg aat ctg gtt gac ttg gct gaa tct gag aga ctg
T L E C C E G N L N L V D L A G S E R L
aag gag tcc ggt tca gaa gga gca aga ctg aca gag aca gag aac ate aca aaa tct ctg
K E S G S E G A R L T E T Q N I N K S L
tcc aat etc ggc aat gtc att atg gca ctt ggt cag aag caa agt cac atc ccc tac cgc
S N L G N V I M A L G Q K Q S H I P Y R
aac tcc aag ctg act cac ctt ctg caa aac tcc ctt ggt ggc aac tcc atg aca ctc atg
N S K L T H L L Q N S L G G N S M T L M
ttt gtc aat gfg tcc ccc ttg gaa atg tgc ttc ggc gag acc ttg aac tet etc cgc ttt
F V N V S P L E M C F G E T L N S L R F
gca acc aag gtc aac cag tgc cac att gga acg get acg aag cac ate agc aaa taa
A T K V N Q C H I G T A T K Q I R K *
agctgatggtggaagattgctgttgcggtgagggattatcctgttggatgtaattatgacagaccctattgaa
taaaagcgattatgctgtaagaggagatcttaagaacattcatttccatttttcttaattttgattttacatctagtgcttc
ctgtatnaattgatactatnaccagactctgfatagctcagtagctgtaccattacaactgtttgcnaataatgatgttagt
tcaataaaaaaaaa

```

**Figure 1. Full-length cDNA of the *kifc1* from the testis of *P. japonicus*.** The corresponding amino acid sequence is shown below the nucleotide sequence. The full-length cDNA of this gene consists of a 136 bp 5' untranslated region, a 297 bp 3' untranslated region and a 2217 bp open reading frame which encodes 738 amino acids.

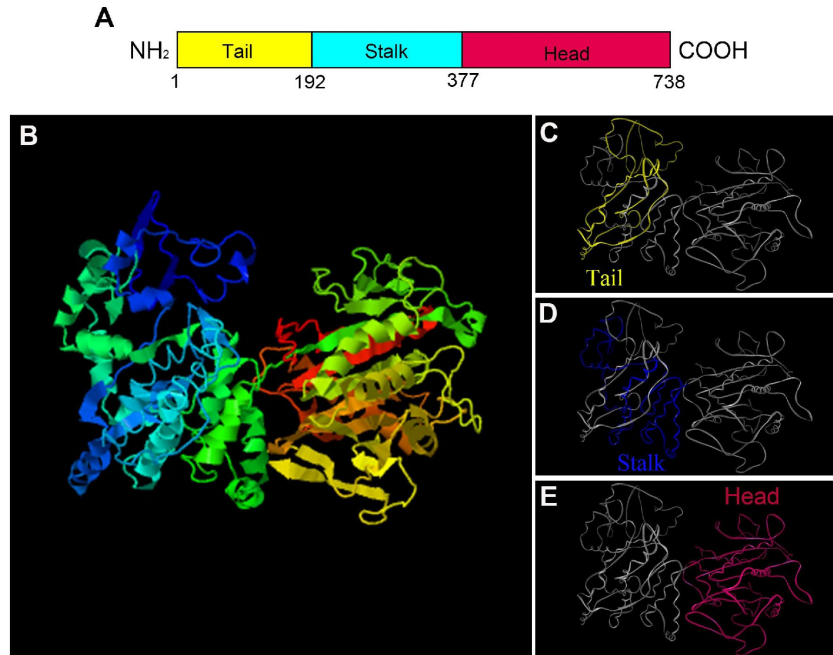


**Figure 2. The prediction of major structural features in *P. japonicus* KIFC1.** (A) Three structural domains of KIFC1 were shown in this figure. The motor domain labeled in red contains the conserved head which is from aa 377 to 738. The stalk region, also named coiled-coil domain, extends from aa 192 to 376 that labels in blue. The divergent tail domain labeled in yellow is from aa 1 to 191. (B) The putative 3-D structure of KIFC1 protein. (C) Tail domain (yellow part). (D) Coiled-coil domain (blue part). (E) Motor domain (red part).

fragment of  $\beta$ -actin were amplified in the heart, hepatopancreas, muscle, gill, was deferens, spermatophore and testis (Figure 5A).  $\beta$ -actin was served as an internal control. Gray analysis by the Image J software indicated that *kifc1* mRNA was extensive expressed in all selected tissues, and the high expression occurred in the testis, vas deferens and spermatophore (Figure 5B). Meanwhile, we identified and analyzed KIFC1 protein expression in muscle, heart, testis, vas deferens and spermatophore by Western blots. A band about 81 kDa was recognized in all of these samples (Figure 5C). The expression trend of KIFC1 protein in all tissues is almost consistent with that of *kifc1* mRNA (Figure 5D), which implies that KIFC1 may have important roles in spermatogenesis of *P. japonicus*.

### KIFC1 participates in mitosis, meiosis as well as spermiogenesis of *P. japonicus*

In order to explore the role of KIFC1 and microtubules during spermatogenesis of *P. japonicus*, we conducted

the immunofluorescence further to examine the localization of them. In the spermatogonial phase, KIFC1 co-localized with tubulin in cytoplasm. Meanwhile, KIFC1 also dispersed in the nucleus (Figure 6A, arrows). In the spermatocyte phase, the signal of KIFC1 and tubulin in cytoplasm was obviously increased when compared with the spermatogonial phase. More importantly, a large number of KIFC1 signal was detected in the nucleus of spermatocyte (Figure 6B, arrows). In the early stage of spermatids, the microtubules began to assemble to one side of the nucleus (Figure 6C, arrows). The KIFC1 signal was exported from the nucleus, and spread over and co-localized with the microtubules in the cytoplasm (Figure 6C, arrows). In the late-stage spermatids, the microtubules exhibited characteristic spindle morphology around the nucleus (Figure 6D, arrows), while the signal of KIFC1 in this phase presented a relative increased (Figure 6D). In the control group, no signal of KIFC1 and tubulin was detected from the spermatogonia to late spermatids (Supplementary Figure 1). These results

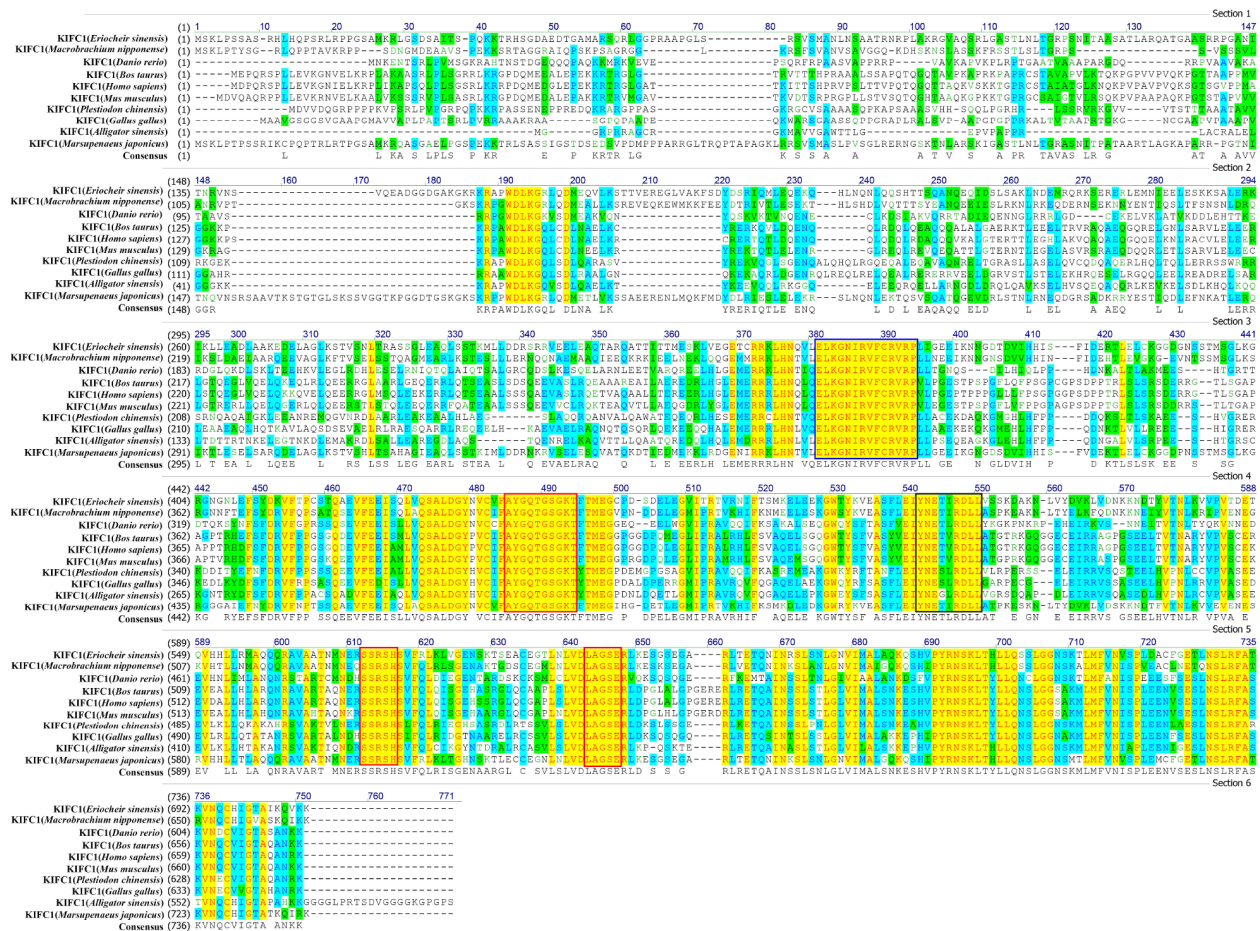


**Figure 3. Multiple sequence alignment of the KIFC1 protein in *P. japonicus* with that of other species.** The ELKGNIRVFCRVP sequence (blue frame) is the KIFC conserved consensus. The AYGQTGSGKT, SSRSH, and LAGSE sequences (red frame) are the putative ATP binding sites. The YNETIRDLL sequence (black frame) is the microtubule-binding site.

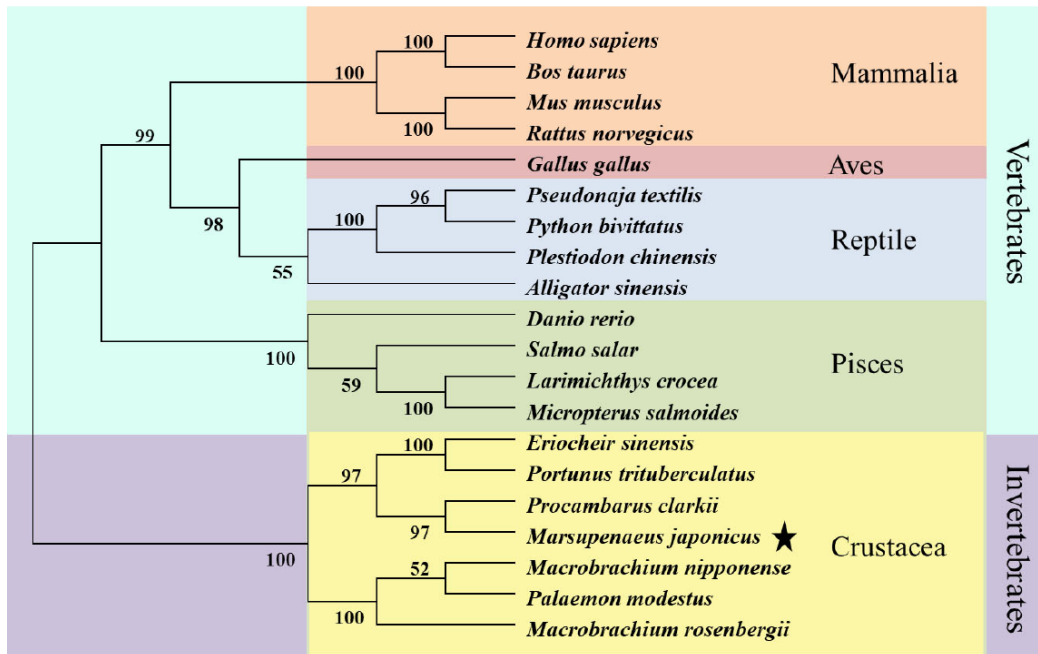


**Figure 4. Phylogenetic tree of KIFC1 protein from different species.** The phylogenetic tree was constructed through the neighbor-joining method with Mega 6 software. Mammalia, Aves, Reptile, Pisces, and Crustacea are included. The putative KIFC1 of *P. japonicus* constitutes a sister clade with it homologues of *Procambarus clarkia*.

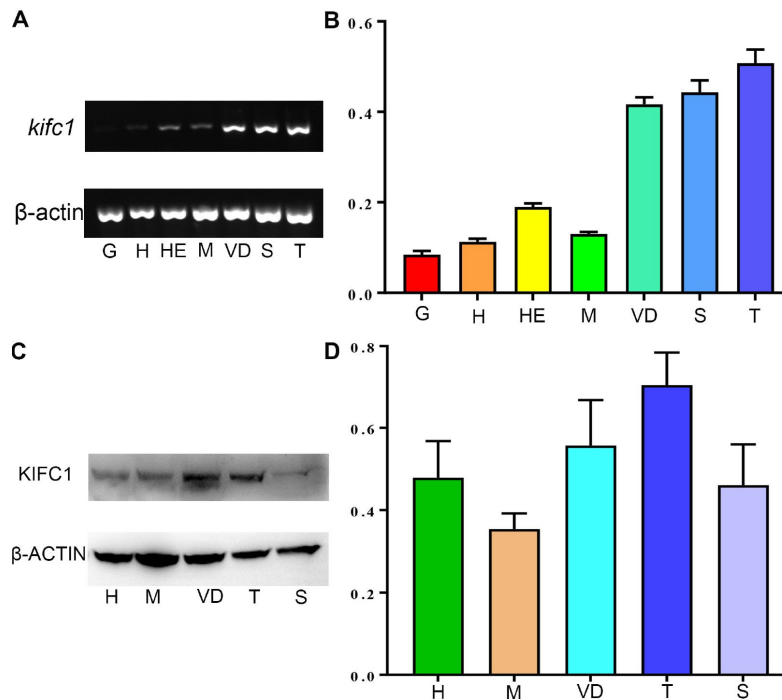


**Figure 5. The expression of KIFC1 in different tissues.** (A) *kifc1* mRNA expression in various *P. japonicus* tissues was shown by semi-quantitative RT-PCR analysis in the upper panel. The lower panel,  $\beta$ -actin, was used as a positive control. (B) A quantitative analysis of *kifc1* mRNA expression in various *P. japonicus* tissues was shown by Image J. The highest expression of *kifc1* appears in the testis. (C) The expression of KIFC1 protein in various *P. japonicus* tissues was shown in the upper panel by western blot. The lower panel,  $\beta$ -actin, was used as a positive control. (D) A quantitative analysis of KIFC1 expression in various *P. japonicus* tissues was shown by Image J. G: gill, H: heart, HE: hepatopancreas, M: muscle, S: spermatophore, T: testis, VD: vas deferens.

suggest that KIFC1 is likely to play essential roles during spermatogenesis of *P. japonicus* including mitosis of spermatogonia, meiosis of spermatocytes and the acrosome formation and maintaining.

During post-spermiogenesis in vas deferens (Figure 7), the microtubules also showed spindle-like structure around the nucleus (Figure 7B, arrows), while the signal of KIFC1 in this phase presented a relative reduction (Figure 7C). In mature sperm from the spermatophore,

we can observe the nucleus, acrosome and spike under phase contrast microscopy (Figure 7I, arrows). The signal of microtubules and KIFC1 was completely not co-localized (Figure 7J, arrows). KIFC1 was localized mainly in the acrosome, but the microtubules were close to the nucleus at the opposite end of acrosome (Figure 7G, 7H, 7J, arrows). These data show that KIFC1 has almost finished its task during spermatogenesis of *P. japonicus*, and continues to maintain the acrosome morphology in mature sperm in spermatophore.

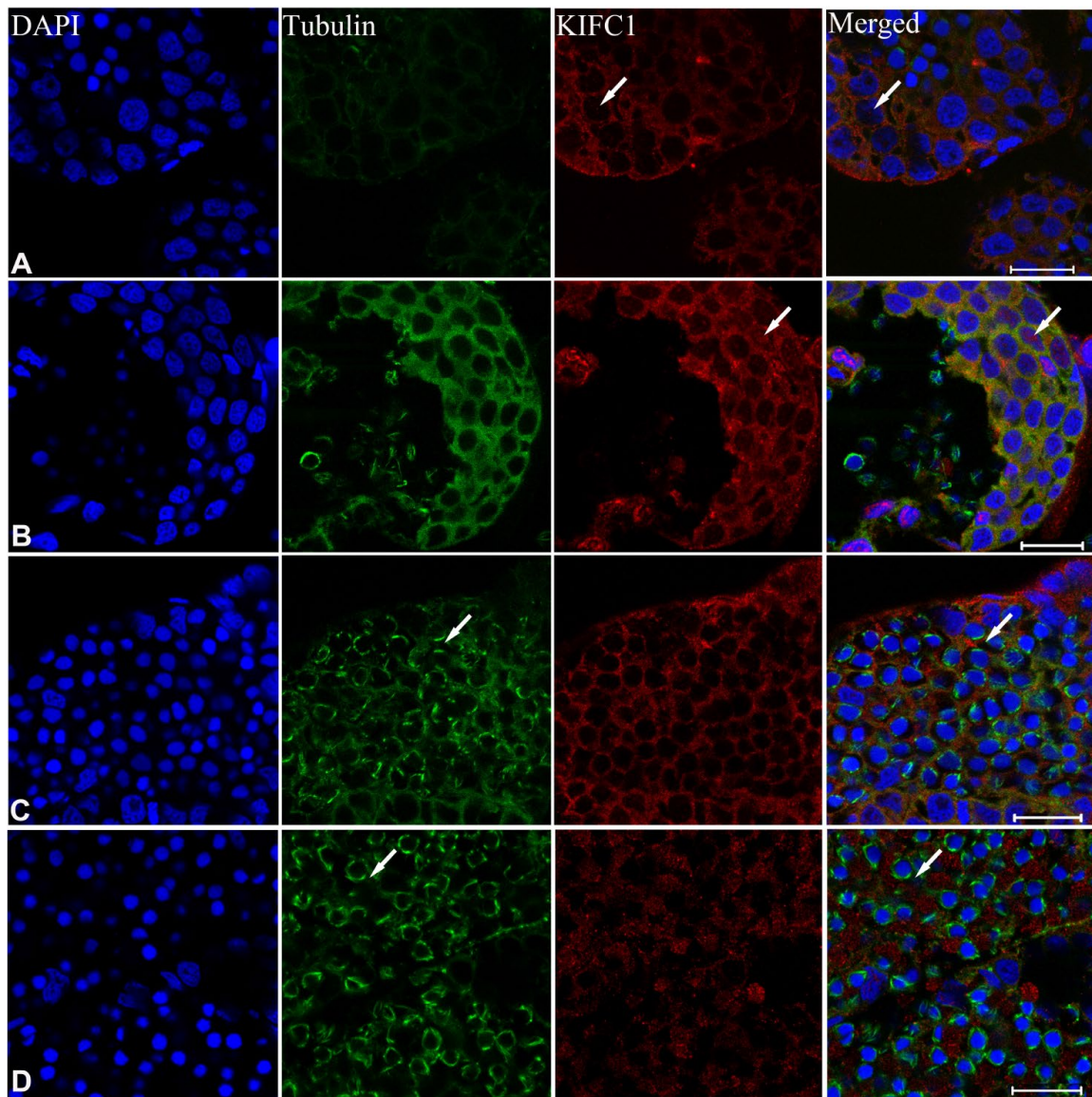


**Figure 6. Immunofluorescent localization of KIFC1 and tubulin during spermatogenesis in the testis of *P. japonicus*.** (A) Spermatogonia. KIFC1 and microtubules were co-localized in the cytoplasm. KIFC1 signal also can be detected in nucleus (white arrows). (B) Spermatocyte. The distribution of KIFC1 and microtubules in spermatocyte was same with that in spermatogonia. The difference was that both KIFC1 and microtubules signal in this stage were increased obviously (white arrows). (C) Early spermatid. KIFC1 and microtubules were distributed in the perinuclear cytoplasm. At this time, the microtubules started to assemble at one end (white arrows). (D) Late spermatid. A mass of KIFC1 spread over the spermatid cytoplasm. The microtubules exhibited spindle morphology around the sperm nucleus (white arrows). Blue: DAPI, Green: tubulin, Red: KIFC1. Scale bar= 20 $\mu$ m.

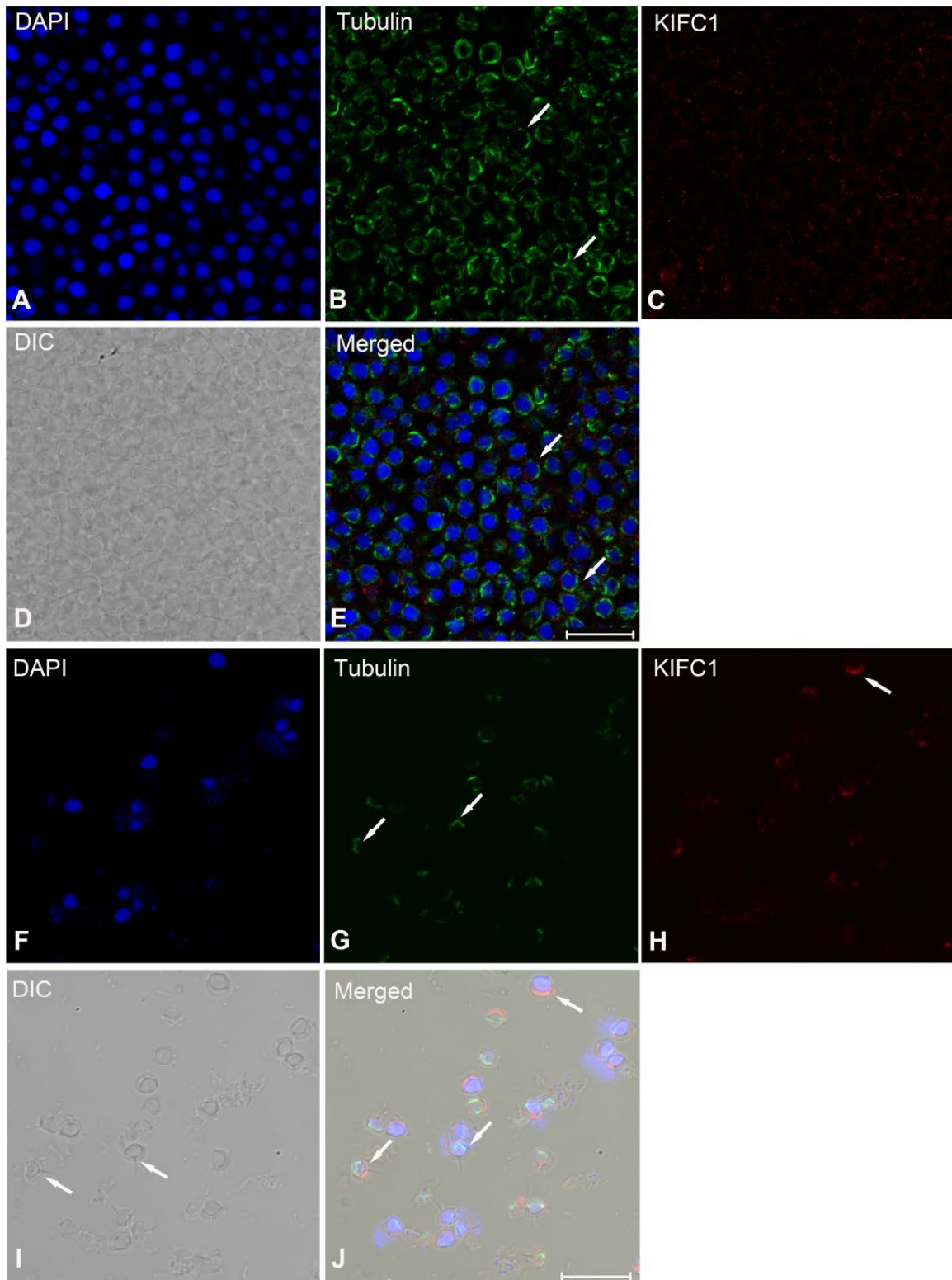


**Figure 7. Immunofluorescent localization of KIFC1 and tubulin during post-spermiogenesis in the vas deferens and in mature sperm from spermatophore of *P. japonicus*.** (A–E) Spermatid during post-spermiogenesis in the vas deferens. The signal of KIFC1 was very weak. The microtubules exhibited spindle morphology around the sperm nucleus (white arrows). (F–J) Mature sperm in spermatophore. KIFC1 and microtubules have completely separated localization in the mature sperm. From (J), it was clearly that KIFC1 was mainly localized at acrosome, while the microtubules distributed in the opposite side cytoplasm. Blue: DAPI, Green: tubulin, Red: KIFC1. Scale bar = 20µm.

## KIFC1 knockdown has a severely impact on microtubule distribution and results in early germ cell apoptosis in the testis of *P. japonicus*

In order to explore the function of KIFC1 during spermatogenesis of *P. japonicus*, we conducted the RNAi experiment through the injection of dsRNA to knockdown the expression of KIFC1 *in vivo*. The knockdown efficiency of *kifc1* was examined by semi-quantitative RT-PCR and Western blot (Figure 8A–8D). From the results of gray analysis, both dsKIFC1-1 and dsKIFC1-2 group had a significantly lower *kifc1* mRNA and KIFC1 protein expression than those of control groups (Figure 8B, 8D). Therefore, both of these two RNAi groups are feasible for further studies.

To determine whether there are effects on microtubule assembly, we observed the distribution of microtubules in the dsKIFC1-1 testis, vas deferens and spermatophore. In the dsKIFC1-1 testis, the signal of KIFC1 is hardly detectable. At the same time, the microtubule signal has an obvious decrease and it presents an abnormal accumulation in spermatogonia (Figure 9A, and Supplementary Figure 2A). However, in the dsKIFC1-1 vas deferens and spermatophore, although KIFC1 expression is knocked down, the expression and distribution of microtubules are not

affected (Figure 9B, 9C, and Supplementary Figure 2B, 2C). These results indicate that KIFC1 knockdown has a serious influence on the distribution of microtubules during the early spermatogenesis of *P. japonicus* including mitosis and meiosis, but not in the late stage, spermiogenesis.

In order to examine the effect of KIFC1 knockdown on spermatogenesis in *P. japonicus*, we conducted TUNEL assay. In the control groups (Normal and dsEGFP testis), no apoptosis is detected (Figure 10A, 10B). But the different results occur in the RNAi groups. Plenty apoptosis is detected in dsKIFC1-1 testes (Figure 10C), and apoptosis is taken place in spermatogonia and spermatocytes at high magnification (Figure 10F). In addition, we also detected apoptosis in the RNAi vas deferens and spermatophore, but the result shows that KIFC1 knockdown has no effect on the spermatids in vas deferens and the mature sperm in spermatophore, which is identical with that of microtubule assembly (Figure 10D, 10E).

## DISCUSSION

Numerous studies have reported that KIFC1 participates in the process of spermatogenesis in both vertebrates and invertebrates and KIFC1 is essential for acrosomal

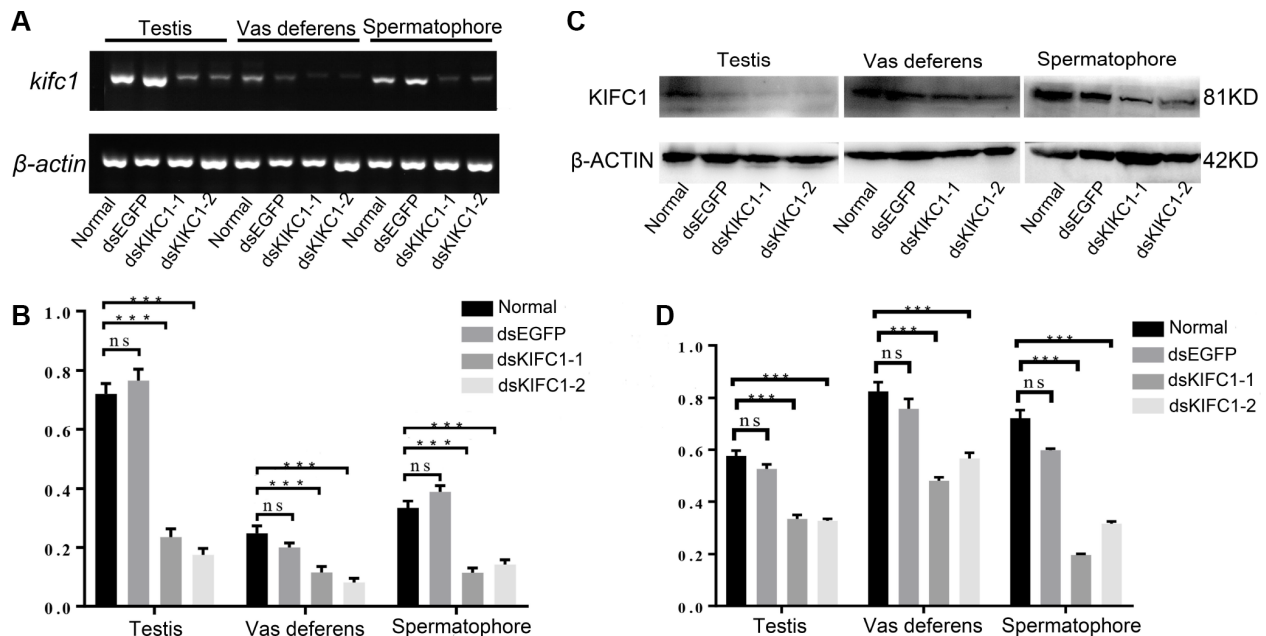


**Figure 8. Knockdown efficiency of *kifc1* by dsRNA injection *in vivo*.** (A) Expression level of *kifc1* mRNA was assayed by semi-quantitative RT-PCR analysis in the testis, vas deferens and spermatophore of *P. japonicus*. (B) A quantitative analysis of *kifc1* mRNA expression in the testis, vas deferens and spermatophore was determined by Image J. (C) Expression level of KIFC1 protein was detected by Western blot in the testis, vas deferens and spermatophore of *P. japonicus*. (D) A quantitative analysis of KIFC1 protein expression in the testis, vas deferens and spermatophore was determined by Image J.  $\beta$ -actin was used as an internal control.



biogenesis and nuclear reshaping [17, 33, 37, 38]. However, there is no study on functions of KIFC1 during spermatogenesis of the species of Penaeidae until nowadays. In this paper, we suggest that KIFC1 has a critical role in spermatogenesis of the penaeid prawns by the spatial and temporal distribution exploring and RNA interference *in vivo*. The results of the spatial and temporal distribution imply that KIFC1 may have a crucial function in mitosis, meiosis and acrosome biogenesis. Further study on the function of KIFC1 through RNA interference *in vivo* showed that KIFC1 knockdown induced spermatogonia and spermatocyte apoptosis, which gave a strong evidence for KIFC1 function in mitosis and meiosis during spermatogenesis of *P. japonicus*.

### **KIFC1 depletion affects the distribution of microtubules and induces the early germ cell apoptosis during spermatogenesis of *P. japonicus***

KIFC1 transports various cargos, including membrane-bounded organelles, vesicles and interacting proteins,

along the microtubule from the plus end to the minus end [30, 39]. Additionally, since the KIFC1 contains a conserved nuclear localization signal in the tail domain, it can be transferred into the nucleus and participates in the regulation of mitosis and meiosis [40–42].

The mitotic and meiosis spindles are molecular machines composed of a bipolar array of microtubules, which contributes to chromosome segregation via microtubule sliding, growth as well as microtubule shrinkage [42, 43]. KIFC1 participates in spindle assembly and modulates spindle length [44]. In many kinds of cancer cells, KIFC1 has been demonstrated playing an essential role in bipolar spindle formation by clustering the multiple poles and maintaining chromosomal stability [45, 46]. Therefore, KIFC1 is closely associated with the dynamic of microtubules during both mitotic and meiosis. In order to explore whether KIFC1 knockdown has an impact on the microtubule dynamic during spermatogenesis of *P. japonicus*, we conducted RNA interference by dsRNA injection *in vivo*. From our results, decreased expression

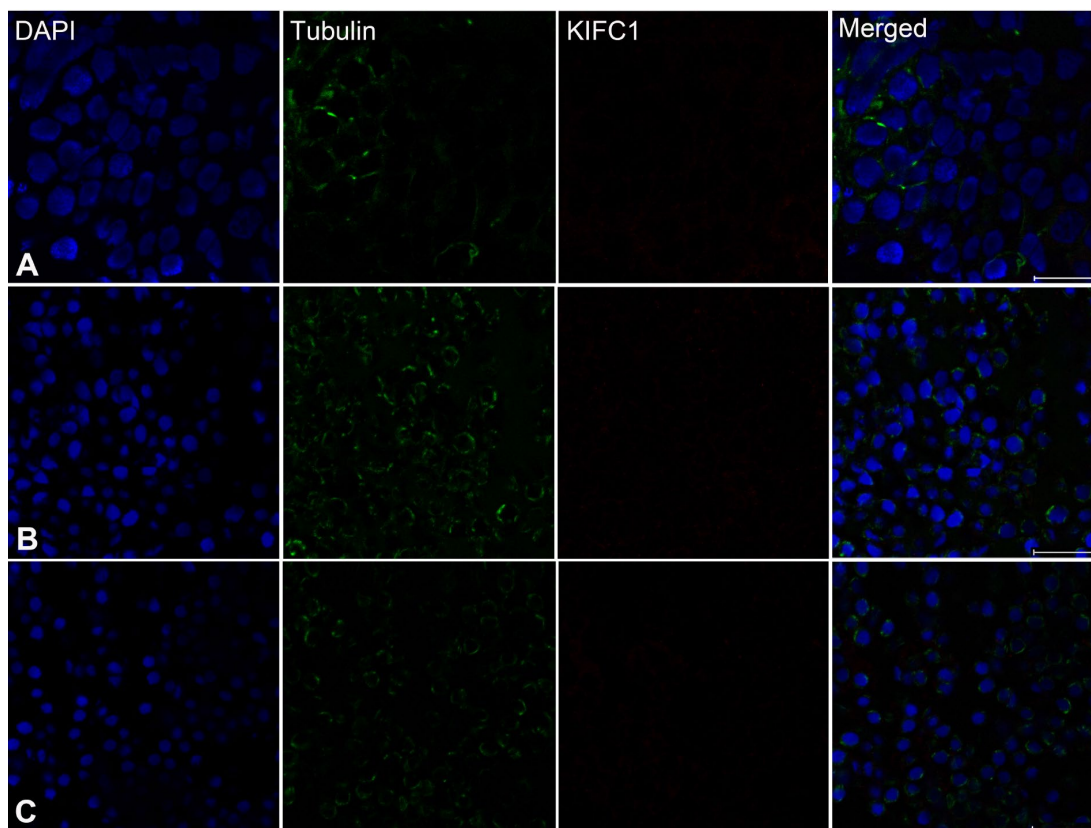


**Figure 9. Effects of *kifc1* knockdown on the distribution and assembly of the microtubules in the testis, vas deferens and spermatosphere. (A) The microtubules in the testis. (B) The microtubules in vas deferens. (C) The microtubules in spermatosphere. When *kifc1* was knockdown, the microtubules were low expressed and abnormally assembled in spermatogonia and spermatocyte, while no obvious difference was found in spermatid from the vas deferens and mature sperm from spermatosphere. Blue: DAPI, Green: tubulin, Red: KIFC1. Scale bar = 20µm.**

of KIFC1 leads to low microtubule signal and abnormal accumulation just in the early stages of spermatogenesis in *P. japonicus* testis. We speculated that the main reason for this phenomenon may be that special morphology assembled by microtubules has been accomplished before spermatids were released into the vas deferens (Figure 9).

KIFC1 is essential for mitosis not only in normal cells, but also in cancer cells. The KIFC1 deficiency affects the normal mitosis, as well as damages cell growth, proliferation and survival. Wei and Yang [47] found that the KIFC1 knockout 293T cells are hard to heal from scratched mechanical damage and cell death occurs in the wound healing assay. In KIFC1-depleted IMR-90 cells, although no obvious immediate cell death was observed, 20% less cells were detected compared with control group. Interestingly, when knocked down both KIFC1 and Mad2 in IMR-90 cells, the cell apoptosis was triggered suggesting their combined effect during mitosis [45]. KIFC1 presents upregulated

in various cancer cells and is related to cancer progression [31, 48, 49]. Besides, the overexpression of KIFC1 can inhibit docetaxel-mediated apoptosis in breast cancer cells and prostate cancer cells [49, 50]. Several studies have shown that KIFC1 is associated with an apoptosis pathway, and inhibition of KIFC1 suppresses cell proliferation, but also induces the apoptosis pathway in different cancer cells [31, 49, 51]. In our study, we determined that cell apoptosis commonly occurred in the spermatogonia of the KIFC1 knockdown testis, which suggested the key function of KIFC1 in mitosis of spermatogonia and KIFC1 depletion resulting in spermatogonia apoptosis in *P. japonicus* (Figure 10).

In meiotic germ cells, KIFC1 also has a role in the regulation of spindle morphology and length, and in chromosome alignment and segregation. KIFC1 inhibition in mouse oocytes leads to aberrant spindle assembly and finally generates meiosis arrest [52]. Ncd, a KIFC1 orthologue in *Drosophila*, is reported to form the

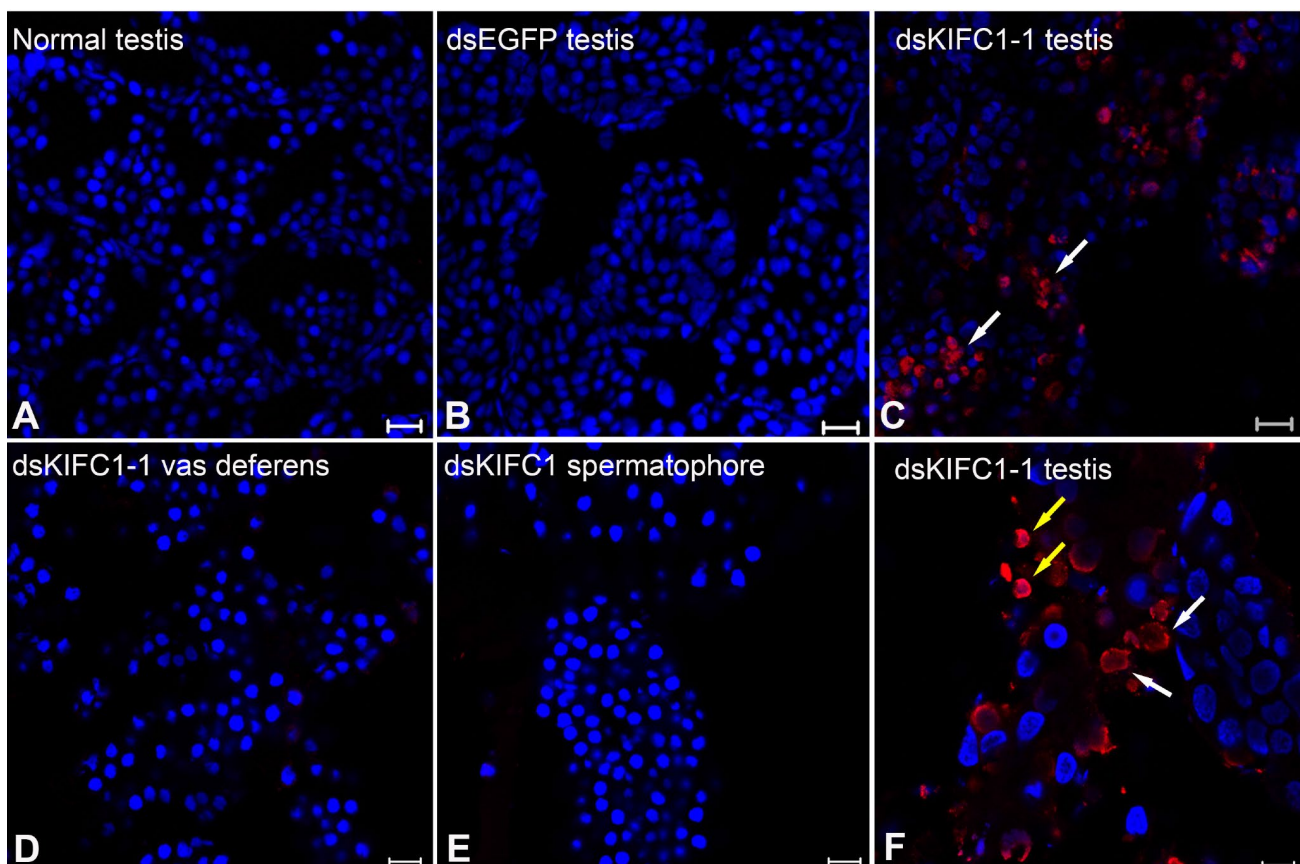


**Figure 10. Effects of *kifc1* knockdown on *P. japonicus* testis detected using the TUNEL assay. (A)** No apoptosis signal was detected in the normal testes. **(B)** No apoptosis signal was detected in dsEGFP testes. **(C)** Apoptosis signal was detected in dsKIFC1-1 testes. **(D)** No apoptosis signal was detected in dsKIFC1-1 vas deferens. **(E)** No apoptosis signal was detected in dsKIFC1-1 spermatophore. **(F)** In dsKIFC1-1 testes, apoptosis was taken place in spermatogonia (white arrows) and spermatocytes (yellow arrows). Blue: DAPI, Red: TUNEL. Scale bar = 20µm in A, B and C. Scale bar = 10µm in D, E and F.

microtubule nucleating center at the spindle pole body during meiosis in oogenesis [53, 54]. In addition, KIFC1 depletion in *Procambarus clarkii* causes a whole suppression of spermiogenesis, which is speculated for the abnormal early spermatids undergo apoptosis due to an unsuccessful meiosis, or as a result of incomplete structure in KIFC1 knockdown testis [55]. All these results suggested that *kifc1* ablation resulted in the normal meiosis interruption or finally induced apoptosis in germ cell genesis [54, 55]. In this study, we detected that in the spermatocyte phase, the signal of KIFC1 and tubulin was obviously increased in cytoplasm by immunofluorescence. Besides, abundant KIFC1 molecules were transported into the nucleus, which implied its importance for normal meiosis of male *P. japonicus* (Figure 6B, arrows). Further analysis of the function of KIFC1 by TUNEL assays showed that KIFC1 knockdown triggered cell apoptosis in spermatocyte phase (Figure 10), which gave the evidence for its important role in normal meiosis during spermatogenesis of *P. japonicus*. Since no available germ cell lines of crustacean, we can't conduct the experiments *in vitro* and explain the effects more clearly. However, our results are still very important.

#### **KIFC1 functions in the acrosome formation and nuclear morphogenesis during spermiogenesis**

The motor protein KIFC1 has been proved to function in the formation of acrosome and morphogenesis of the nucleus in different species from lower animals like invertebrates to mammals (Table 1). It is related to the nuclear membrane and acrosome in round and elongating spermatids in mammal [56]. In rats, KIFC1 may combine with nuclear factors and contribute to the formation of spermatid acrosome, as well as the nuclear changes, which gives the direct association of a molecular motor with the acrosome biogenesis and nuclear morphogenesis [17]. Wang et al. [32] came up with the initial hypothesis that KIFC1 keep the conserved role during spermiogenesis of cephalopods: participating in acrosome formation and nucleo-morphogenesis. And then, they detected that *kifc1* mRNA signal was abundant in spermatid undergoing acrosome formation and dramatic elongation in *Octopus tankahkeei*. In addition, during nuclear elongation and condensation KIFC1 was completely co-localized with the cephalopod counterpart of manchette. It suggested that cephalopod KIFC1 took part in nuclear morphogenesis with assisting of the manchette-like perinuclear microtubules to transport specific cargoes [57]. During the swimming crab spermiogenesis such as *Portunus trituberculatus* and *Eriocheir sinensis*, several studies also have provided a preliminary evidence for the essential roles of KIFC1 in the acrosome biogenesis and nuclear morphogenesis [33, 37, 58]. However, in the phylum Sipuncula

*Phascolosoma esculenta*, there is something different. Combined the detailed observations of the dynamic distribution of motor protein KIFC1, microtubules and mitochondria during spermiogenesis with the conserved function of KIFC1 in cargo transport and microtubule organization, the researchers proposed that KIFC1 functions in nuclear reshaping and midpiece formation in the spermiogenesis of *P. esculenta* [35].

The Natantia species of Decapoda is divided into three tribes: Caridea, Penaeid and Stenopodidea. In Caridea, several studies have been reported about KIFC1 participating in the spermiogenesis. Acroframosome (AFS) is a new structure consisted of microtubules, which is identified from *M. nipponense*. The microtubule bundle of AFS started from middle stage spermatids and localized around the developing acrosome, which assembled in an everted umbrella [38]. KIFC1 was then notarized to transport cargoes such as Golgi vesicles, mitochondria and other cellular components that results in acrosome formation and nuclear shaping with the help of AFS during the spermiogenesis of *Exopalaemon modestus* [59]. During *P. clarkii* spermiogenesis, although the AFS was not reported, there is no effect on KIFC1 functions in acrosome formation and nuclear shaping [55]. In this study, the KIFC1 randomly dispersed in the cytoplasm, and co-localized with the microtubules in early stage spermatid of *P. japonicus*, which is similar with that of *P. clarkia*, *M. nipponense* and *E. modestus* [38, 55, 59]. In the late-stage spermatids, the microtubules exhibited characteristic spindle morphology around the nucleus, while the signal of KIFC1 in this phase presented a relative reduction. In mature sperm from the spermatophore, the nucleus, acrosome and spike were clearly observed by phase contrast microscopy. The signal of microtubules and KIFC1 was completely separated. KIFC1 was localized mainly in the acrosome, but the microtubules were close to the nucleus in the opposite end of acrosome. This is a novel phenomenon, which has not reported in other species. We proposed that since sperm stored in spermatophore were completely mature, and what they need to do is just waiting for fertilization, the motor protein KIFC1 and microtubules have finished their mission. Owing to the limit of the interference duration and survival time after injection which are the two main factors influenced the outcome of this study, it is hardly for us to observe the morphological abnormality and to obtain the direct evidence for more specific function of KIFC1 in the acrosome formation and nuclear morphogenesis.

#### **CONCLUSIONS**

In this study, we concentrated on the KIFC1 function in spermatogenesis of *P. japonicus*, and tried to uncover the reproduction and regulation mechanism. The

**Table 1. The functions of the motor protein KIFC1 in spermatogenesis of various species.**

Species	Effect stage	Cell type	Function	Reference
Rat	Spermiogenesis	Spermatid	Transport vehicles; Acrosome formation	[17]
<i>Xenopus laevis</i>	Mitosis	Spermatogonia	Spindle bipolarity	[19]
<i>Eumeces chinensis</i>	Spermiogenesis	Spermatid	Acrosome biogenesis, nucleus reshaping and tail formation related	[60]
<i>Gekko japonicus</i>	Spermiogenesis	Spermatid	Acrosome formation; nuclear reshaping	[34]
<i>Larimichthys crocea</i>	spermiogenesis	Spermatid	Nuclear reshaping; flagellum formation	[61]
<i>Drosophila</i>	Meiosis	Oocyte	Meiosis II spindle assembly	[53]
<i>Marsupenaeus japonicus</i>	Mitosis; meiosis; spermiogenesis	Spermatogonia; spermatocyte; spermatid	Participate in mitosis and meiosis; Regulate microtubule assembly; Acrosome biogenesis and maintaining	The present study
<i>Eriocheir sinensis</i>	Spermiogenesis	Spermatid	Acrosome biogenesis and its maintenance	[37, 39]
<i>Octopus tankahkeei</i>	Spermiogenesis	Spermatid	Cytological transformation; sperm nuclear morphogenesis	[32, 57]
<i>Macrobrachium nipponense</i>	Spermiogenesis	Spermatid	Acrosome biogenesis; cellular transformation	[38]
<i>Exopalaemon modestus</i>	Spermiogenesis	Spermatid	Acrosome formation; nuclear shaping	[59]
<i>Portunus trituberculatus</i>	Spermiogenesis	Spermatid	Acrosome biogenesis; nuclear shaping	[33]
<i>Procambarus clarkii</i>	Spermiogenesis	Spermatid	Acrosome formation; nuclear shaping	[55]
<i>Phascolosoma esculenta</i>	Spermiogenesis	Spermatid	Nuclear reshaping; midpiece formation	[35]

temporal and spatial expression patterns of KIFC1 protein during spermatogenesis indicates that KIFC1 is likely to participate in the mitosis of spermatogonia, meiosis of spermatocyte, acrosome formation during spermiogenesis and acrosome maintaining in mature sperm. Besides, the result of KIFC1 knockdown by dsRNA injection verifies that deficiency KIFC1 causes aberrant microtubule expression and distribution, and also results in spermatogonia and spermatocyte apoptosis in the testes. In summary, our results provide a strong evidence for the important roles of KIFC1 during *P. japonicus* spermatogenesis. Because it's hard to generate gene knockout crustacean by now, we attempted to knock down KIFC1 by dsRNA injection to elucidate its function during spermatogenesis *in vivo*, and its feasibility was verified. We hope this method could help to solve more scientific issues in crustacean study and other field.

## MATERIALS AND METHODS

### Animals and sample preparation

The adult male Kuruma shrimp were purchased from the aquatic market of Luoja Village in Hangzhou city (Zhejiang, China). We quickly sacrificed these shrimps and dissected to collect the heart, hepatopancreas, muscle, gill, epididymis, spermatophore and testis on ice. The detached heart, hepatopancreas, muscle, gill

were put into liquid nitrogen immediately and then preserved at  $-80^{\circ}\text{C}$  for RNA and protein extraction. The detached tissues of epididymis, spermatophore and testis were saved in two parts. One part was stored in  $-80^{\circ}\text{C}$  for RNA and protein extraction. The other part was fixed in 4% paraformaldehyde (PFA) in phosphate buffered saline (PBS, 0.1 M, pH 7.4) at  $4^{\circ}\text{C}$  overnight, then dehydrated in 20% sucrose solution in PBS for 8 h and embedded with O.C.T. for immunofluorescence. These samples were stored at  $-40^{\circ}\text{C}$ .

### RNA extraction and reverse transcription

Total RNA of the heart, hepatopancreas, muscle, gill, epididymis, spermatophore and testis were extracted according to the manufacturer's instructions of Trizol reagent (Takara, Dalian, China). All samples were dissolved and homogenized within the Trizol reagent by a homogenizer. The homogenate was sequentially dealt with chloroform, isopropanol and 75% ethanol to make the RNA precipitated. Finally, we dissolved the precipitated RNA from each tissue in 100  $\mu\text{l}$  DEPC- $\text{H}_2\text{O}$  and measured its concentration by micro-spectrophotometer (Nano-100, Allsheng). All total RNA samples were stored at  $-80^{\circ}\text{C}$ .

The PrimeScript® RT reagent Kit (Takara) was used to reverse transcript the total RNA into cDNA. All samples were stored at  $-20^{\circ}\text{C}$  for semi-quantitative

PCR analysis of KIFC1 mRNA expression in different tissues. In addition, the testis cDNA was used for *kifc1* gene cloning. The Smart RACE cDNA Amplification Kit (CloneTech) and the 3'-Full RACE Core Set with PrimeScript™ RTase (Takara) were used for 5' and 3' rapid-amplification of cDNA ends (RACE) reverse transcription, respectively.

### Full-length of *kifc1* cloning

It was reported that kinesin protein KIFC1 is conserved in its C-terminal. Thus, we try to design two pairs of primers (Table 2) based on the conserved region of *kifc1* from *Eriocheir sinensis* by using the Primer Premier 5 software to get the conserved sequence of the shrimp *kifc1* in the testis. All the primers were synthesized by the Shanghai Sangon Biological Engineering Technology Company (China). A cDNA fragment of *kifc1* was obtained by Nested Touchdown PCR using a Mygene Series Peltier Thermal Cycler (Hangzhou, China). The program ran as follows: 94°C for 5 min, 10 cycles of the touchdown program (94°C for 30 s, 55°C for 30 s, 72°C for 1.5 min, followed by 0.5°C decrease of the annealing temperature per cycle), followed by 25 cycles (94°C for 30 s, 50°C for 30 s, and 72°C for 1.5 min), and 10 min at 72°C for the final extension. The PCR products were then determined and separated by agarose electrophoresis. SanPrep column DNA gel extraction kit (Sangon Biotech) was used to purify the desired bands. Eventually, the purified fragment was linked into PMD19-T-vector (Takara), propagated in *Escherichia coli* DH5 $\alpha$  (Takara) and then sent to the Sangon Biological Engineering Technology Company for sequencing.

Based on this determined sequence, we designed two forward primers (3'F1 and 3'F2) for 3' RACE and one reverse primer (5'R1) for 5' RACE using the Primer Premier 5 software. Then we performed the Nested Touchdown PCR with the reverse primers from the 3'-Full RACE Core Set with PrimeScript™ RTase to obtain the 3' RACE, and with the forward primer from the Smart RACE cDNA Amplification Kit (CloneTech) to get the 5' RACE. We ran the 3' RACE programs as follows: 94°C for 5 min, 10 cycles of the touchdown program (94°C for 30 s, 62°C for 30 s, 72°C for 0.5 min, followed by 0.5°C decrease of the annealing temperature per cycle), followed by 25 cycles (94°C for 30 s, 57°C for 30 s, and 72°C for 0.5 min), and 10 min at 72°C for the final extension. The 5' RACE programs was as follows: 94°C for 5 min, 10 cycles of the touchdown program (94°C for 30 s, 68°C for 30 s, 72°C for 0.5 min, followed by 0.5°C decrease of the annealing temperature per cycle), followed by 25 cycles (94°C for 30 s, 63°C for 30 s, and 72°C for 0.5 min), and 10 min at 72°C for the final extension. The aimed

PCR products were purified, amplified and sequenced by Sangon Biological Engineering Technology Company as described above.

### Sequence analysis and phylogenetic analysis

The full-length KIFC1 cDNA sequence was checked and assembled by Seqman (DNASTAR, Inc.). The amino acid sequence was translated by the online ExpAsy translate tool (<http://web.expasy.org/translate/>). Multiple sequence alignments were performed with Vector NTI10 (Invitrogen). The secondary structure of KIFC1 protein was predicted with an online tool PSIPRED Workbench (<http://bioinf.cs.ucl.ac.uk/psipred/>). The 3-D structure of KIFC1 was predicted with an online server I-TASSER (<http://zhanglab.ccmb.med.umich.edu/I-TASSER>). The phylogenetic tree, neighbor-joining (NJ) method, was constructed according to the deduced amino acid sequence using MEGA 6. The aa sequence of KIFC1 homologues used in this study was downloaded from NCBI. Their Genbank accession numbers were as follow: *Homo sapiens* (NP\_002254.2), *Bos taurus* (NP\_001095406.1), *Mus musculus* (NP\_001182227.1), *Rattus norvegicus* (NP\_001005878.1), *Gallus gallus* (NP\_001075167.1), *Pseudonaja textilis* (XP\_026580999.1), *Python bivittatus* (XP\_007442391.1), *P. chinensis* (AFP33411.1), *Alligator sinensis* (XP\_006032359.1), *Danio rerio* (NP\_571281.2), *Salmo salar* (ABQ59663.1), *Larimichthys crocea* (ALP83460.1), *Micropterus salmoides* (AKS36882.1), *E. sinensis* (ADJ19048.1), *Portunus trituberculatus* (AKS36885.1), *P. clarkii* (AJF36162.1), *M. nipponense* (AFP33456.1), *Palaemon modestus* (AIN36847.1), and *M. rosenbergii* (AFO63546.1).

### Semi-quantitative PCR analysis of KIFC1 mRNA expression

A pair of primers (KIFC1-RTF1, KIFC1-RTR1) (Table 2) were designed for analyzing the expression of KIFC1 mRNA in different tissues: heart, hepatopancreas, muscle, gill, seminiferous duct, spermatophore and testis. A pair of primers (actin-F1, actin-R1) (Table 2) was used to amplify a  $\beta$ -actin cDNA fragment as the control. The PCR program was run as follows: initial incubation at 94°C for 5 min; 35 cycles in a normal program: 94°C for 5 s, 60°C for 10 s, and 72°C for 15 s; 72°C for 5 min for the final extension. The software Image J was used to analyze the expression of KIFC1 mRNA in different tissues.

### Western blot

All tissues were homogenized in RIPA Lysis Buffer (Beyotime) with 1% protease inhibitors. The total protein was separated by 10% SDS-PAGE gels and then

**Table 2. Primers used in *kifc1* cloning, semi-quantitative RT-PCR, and recombinant plasmid construction for dsRNA synthesis.**

Primer	Primer sequence	Purpose
F1	GCVYTNGAYGGYTAYAAAYGTSTG	PCR
R1	TTNGAGTTDCCDCCVAGRGA	PCR
F2	TATGGNCARACHGGHTCDGG	PCR
R2	CCRGCSARRTCHACMARRTT	PCR
3'F1	GGCTCAAACCTCACAGGGCACAA	3' RACE
3'F2	TGTTTCATCACCTCCTGACGCTT	3' RACE
5'R1	GACATTGCCGAGATTGGACAGAGATTTG	5' RACE
KIFC1-RTF1	TGTCAAAGTCATCTGTGGGAGG	Semi-quantitative RT-PCR
KIFC1-RTR1	TATCTGGCGTTCAAGTGTGGC	Semi-quantitative RT-PCR
actin-F1	AGCCTTCCTTCTGGGTATGG	Semi-quantitative RT-PCR
actin-R1	AGGGAGCGAGGGCAGTGATT	Semi-quantitative RT-PCR
dsKIFC1-F1	GGACTAGTGGGCTGGAGATACAAGGTAGAGG	Plasmid construction
dsKIFC1-R1	CCGCTCGAGAAGGGGGACACATTGACAAACAT	Plasmid construction
dsKIFC1-F2	GGACTAGTCTGTCAAAGTCATCTGTGGGAGG	Plasmid construction
dsKIFC1-R2	CCGCTCGAGTATCTGGCGTTCAAGTGTGGC	Plasmid construction
dsGFP-F1	GGACTAGTCGACGTAACGGCCACAAGTT	Plasmid construction
dsGFP-R1	CCGCTCGAGATGGGGGTGTTCTGCTGGTAG	Plasmid construction

transferred to PVDF membranes (Millipore) by 200 mA, 90 min. After 2 h blocked with 5% non-fat milk in PBST buffer (0.1% Tween-20 in PBS, pH 7.2-7.4), the membranes were incubated overnight in primary antibodies at 4 °C (KIFC1 rabbit polyclonal antibody (1:500) designed and prepared by our lab, anti-ACTB rabbit polyclonal antibody (1:2000, BBI)). We washed the membranes in PBST (three times, 15min/time). Then the membranes were incubated with secondary goat-anti-rabbit HRP-conjugated antibody (1:4000, Beyotime) for 1h. After washing three times with PBST, an enhanced chemiluminescent kit (Beyotime) was used to examine the protein blots by chemiluminescence imaging.  $\beta$ -actin was used as control.

### Immunofluorescence

The samples were taken out from -40°C and cut into 8  $\mu$ m sections with Cryostat microtome (Thermo Scientific, HM525 NX). The sections were permeabilized with 0.25% Triton X-100 in PBS for 15 min. Then, 5% BSA in PBST buffer was used to block the sections for 1 h. After that, the sections were incubated with KIFC1 rabbit polyclonal antibody (1:100) overnight at 4 °C. The negative control sections were incubated in 5% BSA without primary antibody. They were washed in PBST for 45 min (3 times, 15 min/time). Subsequently, the sections were incubated with Secondary Alexa Fluor 555-conjugated donkey-anti-rabbit antibody (1:500, Beyotime) and anti- $\alpha$ -Tubulin-FITC mouse monoclonal antibody (1:100, Sigma) at room temperature for 1 h. The negative

control sections were incubated with just Secondary Alexa Fluor 555-conjugated donkey-anti-rabbit antibody (1:500, Beyotime). After washed 3 times like before, the sections were incubated with DAPI (Beyotime) for 5 min to stain the nucleus. Finally, the sections were mounted with Antifade Mounting Medium (Beyotime) and observed immediately with a confocal laser scanning microscope (Carl Zeiss, CLSM 710).

### RNA interference (RNAi)

Two pairs of specific primers of *kifc1* and one pair of EGFP negative control primers (Table 2) with restriction sites SpeI/ XhoI were designed by the Primer Premier 5 software. We cloned the target sequences into L4440 plasmid with two T7 promoters. The recombinant plasmid was used as template to synthesize the dsRNA by T7 RNAi Transcription kit (Vazyme). We examined the quality and concentration of dsRNA by 1% agarose gel electrophoresis and a microspectrophotometer (Nano-100, Allsheng), respectively.

The active adult male shrimps were selected for the RNA interference experiment. All selected shrimps were divided into four groups (Normal group, dsEGFP group, dsKIFC1-1 group and dsKIFC1-2 group, 12 individuals in each group) and cultured under a stationary temperature of 18°C in separated boxes. After the shrimps were adapted to the environment of the laboratory for 1 week, *in vivo* injections of dsRNA were given. Each shrimp was injected with 20 $\mu$ g dsRNA in

20 µl RNase-free water every three days, and lasted for two weeks. There was no treatment in normal group.

### TUNEL assay

The One Step TUNEL Apoptosis Assay Kit (Beyotime) was used for TUNEL assays. The prepared sections were fixed in 4% PFA for 30 min, and then permeabilized in 0.5% Triton X-100 in PBS for 5 min. After washed in PBS for two times, they were incubated with TUNEL reaction mixture for 1 h at 37 °C away from light, washed for three times in PBS, then stained with DAPI (Beyotime) for 5 min. Finally, the sections were mounted with Antifade Mounting Medium (Beyotime) and observed immediately with a confocal laser scanning microscope (Carl Zeiss, CLSM 710).

### Statistical analysis

Statistical analyses were performed by the GraphPad Prism 7.0 software. The t-test was used to determine the difference between two groups. Statistical significance was presented as \* $p < 0.05$ ; \*\* $p < 0.01$ ; \*\*\* $p < 0.001$ , and no significance (ns). We indicated the results as means  $\pm$  SEM.

### ACKNOWLEDGMENTS

The authors greatly appreciate all members of the Sperm Laboratory in Zhejiang University for their helpful suggestions and discussions on this study.

### CONFLICTS OF INTEREST

The authors declare that there are no conflicts of interest.

### FUNDING

This project was supported by the National Natural Science Foundation of China (No. 41776144 and No. 31572603).

### REFERENCES

- Ahmed EA, de Rooij DG. Staging of mouse seminiferous tubule cross-sections. *Methods Mol Biol.* 2009; 558:263–77. [https://doi.org/10.1007/978-1-60761-103-5\\_16](https://doi.org/10.1007/978-1-60761-103-5_16) PMID:19685330
- Ma DD, Wang DH, Yang WX. Kinesins in spermatogenesis. *Biol Reprod.* 2017; 96:267–76. <https://doi.org/10.1095/biolreprod.116.144113> PMID:28203733
- Hermo L, Pelletier RM, Cyr DG, Smith CE. Surfing the wave, cycle, life history, and genes/proteins expressed by testicular germ cells. Part 2: changes in spermatid organelles associated with development of spermatozoa. *Microsc Res Tech.* 2010; 73:279–319. <https://doi.org/10.1002/jemt.20783> PMID:19941292
- Niksirat H, Kouba A, Rodina M, Kozák P. Comparative ultrastructure of the spermatozoa of three crayfish species: *Austropotamobius torrentium*, *Pacifastacus leniusculus*, and *Astacus astacus* (Decapoda: Astacidae). *J Morphol.* 2013; 274:750–58. <https://doi.org/10.1002/jmor.20132> PMID:23475696
- Feng T, Paterson B, Johnston S. A morphological study of the male reproductive tract, post-testicular acrosome maturation and spermatophore formation in the black tiger prawn (*Penaeus monodon*). *J Morphol.* 2018; 279:1290–300. <https://doi.org/10.1002/jmor.20869> PMID:30117606
- Jamieson BG. Ultrastructure and phylogeny of crustacean spermatozoa. *Mem Queensl Mus.* 1991; 31:109–42.
- Medina A, Mourente G, López de la Rosa I, Santos A, Rodríguez A. Spermatozoal ultrastructure of *Penaeus kerathurus* and *Penaeus japonicus* (Crustacea, Dendrobranchiata). *Zoomorphology.* 1994; 114:161–67. <https://doi.org/10.1007/BF00403263>
- Feng T, Paterson B, Johnston SD. New insights into the spermatogenesis of the black tiger prawn, *Penaeus monodon*. *J Morphol.* 2017; 278:689–703. <https://doi.org/10.1002/jmor.20664> PMID:28164360
- Fransozo V, Fernandes AB, Lopez-Greco LS, Zara FJ, Santos DC. Functional morphology of the male reproductive system of the white shrimp *Litopenaeus schmitti* (Burkenroad, 1936) (Crustacea, Penaeidea) compared to other *Litopenaeus*. *Invertebr Reprod Dev.* 2016; 60:161–74. <https://doi.org/10.1080/07924259.2016.1174158>
- Poljaroen J, Vanichviriyakit R, Tinikul Y, Phoungpetchara I, Linthong V, Weerachatanukul W, Sobhon P. Spermatogenesis and distinctive mature sperm in the giant freshwater prawn, *Macrobrachium rosenbergii* (De Man, 1879). *Zool Anz.* 2010; 249:81–94. <https://doi.org/10.1016/j.jcz.2010.03.002>
- Rotllant G, Chiva M, Durfort M, Ribes E. Internal anatomy and ultrastructure of the male reproductive system of the Norway lobster *Nephrops norvegicus* (Decapoda: astacidea). *J Morphol.* 2012; 273:572–85. <https://doi.org/10.1002/jmor.20002> PMID:22318910
- Stewart MJ, Stewart P, Soonklang N, Linthong V, Hanna PJ, Duan W, Sobhon P. Spermatogenesis in the blue swimming crab, *Portunus pelagicus*, and evidence for histones in mature sperm nuclei. *Tissue Cell.* 2010; 42:137–50.

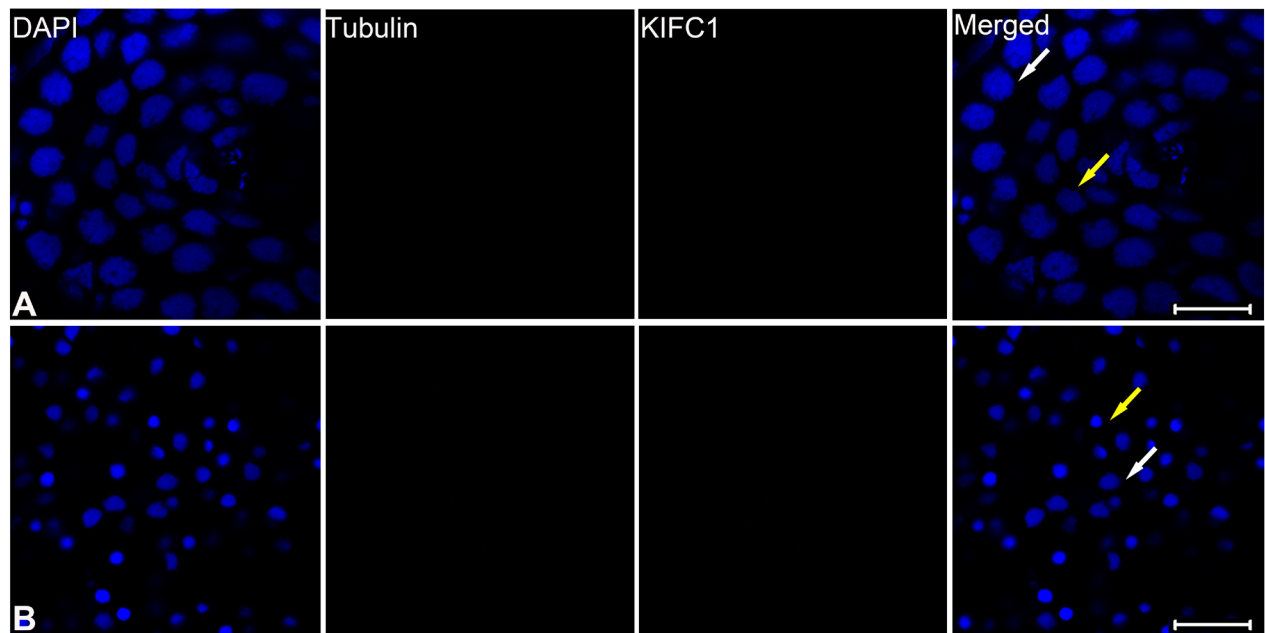
- <https://doi.org/10.1016/j.tice.2010.03.002>  
PMID:20413138
13. Vogt G. Structural specialties, curiosities, and record-breaking features of crustacean reproduction. *J Morphol*. 2016; 277:1399–422.  
<https://doi.org/10.1002/jmor.20582> PMID:27454749
  14. Niksirat H, James P, Andersson L, Kouba A, Kozák P. Label-free protein quantification in freshly ejaculated versus post-mating spermatophores of the noble crayfish *Astacus astacus*. *J Proteomics*. 2015; 123:70–77.  
<https://doi.org/10.1016/j.jprot.2015.04.004>  
PMID:25871631
  15. Xiao X, Yang WX. Actin-based dynamics during spermatogenesis and its significance. *J Zhejiang Univ Sci B*. 2007; 8:498–506.  
<https://doi.org/10.1631/jzus.2007.B0498>  
PMID:17610330
  16. Lehti MS, Kotaja N, Sironen A. KIF1-binding protein interacts with KIF3A in haploid male germ cells. *Reproduction*. 2015; 150:209–16.  
<https://doi.org/10.1530/REP-15-0173> PMID:26245936
  17. Yang WX, Sperry AO. C-terminal kinesin motor KIFC1 participates in acrosome biogenesis and vesicle transport. *Biol Reprod*. 2003; 69:1719–29.  
<https://doi.org/10.1095/biolreprod.102.014878>  
PMID:12826589
  18. Ems-McClung SC, Walczak CE. Kinesin-13s in mitosis: key players in the spatial and temporal organization of spindle microtubules. *Semin Cell Dev Biol*. 2010; 21:276–82.  
<https://doi.org/10.1016/j.semcdb.2010.01.016>  
PMID:20109574
  19. Hentrich C, Surrey T. Microtubule organization by the antagonistic mitotic motors kinesin-5 and kinesin-14. *J Cell Biol*. 2010; 189:465–80.  
<https://doi.org/10.1083/jcb.200910125>  
PMID:20439998
  20. Hu CK, Coughlin M, Field CM, Mitchison TJ. KIF4 regulates midzone length during cytokinesis. *Curr Biol*. 2011; 21:815–24.  
<https://doi.org/10.1016/j.cub.2011.04.019>  
PMID:21565503
  21. Sati L, Seval-Celik Y, Unek G, Korgun ET, Demir R. The presence of kinesin superfamily motor proteins KIFC1 and KIF17 in normal and pathological human placenta. *Placenta*. 2009; 30:848–54.  
<https://doi.org/10.1016/j.placenta.2009.07.005>  
PMID:19679349
  22. Liu XS, Zhao XD, Wang X, Yao YX, Zhang LL, Shu RZ, Ren WH, Huang Y, Huang L, Gu MM, Kuang Y, Wang L, Lu SY, et al. Germinal cell aplasia in Kif18a mutant male mice due to impaired chromosome congression and dysregulated BubR1 and CENP-E. *Genes Cancer*. 2010; 1:26–39.  
<https://doi.org/10.1177/1947601909358184>  
PMID:20981276
  23. Lehti MS, Kotaja N, Sironen A. KIF3A is essential for sperm tail formation and manchette function. *Mol Cell Endocrinol*. 2013; 377:44–55.  
<https://doi.org/10.1016/j.mce.2013.06.030>  
PMID:23831641
  24. Drummond DR. Regulation of microtubule dynamics by kinesins. *Semin Cell Dev Biol*. 2011; 22:927–34.  
<https://doi.org/10.1016/j.semcdb.2011.09.021>  
PMID:22001250
  25. DeBerg HA, Blehm BH, Sheung J, Thompson AR, Bookwalter CS, Torabi SF, Schroer TA, Berger CL, Lu Y, Trybus KM, Selvin PR. Motor domain phosphorylation modulates kinesin-1 transport. *J Biol Chem*. 2013; 288:32612–21.  
<https://doi.org/10.1074/jbc.M113.515510>  
PMID:24072715
  26. Czechanski A, Kim H, Byers C, Greenstein I, Stumpff J, Reinholdt LG. Kif18a is specifically required for mitotic progression during germ line development. *Dev Biol*. 2015; 402:253–62.  
<https://doi.org/10.1016/j.ydbio.2015.03.011>  
PMID:25824710
  27. Mukhopadhyay A, Quiroz JA, Wolkoff AW. Rab1a regulates sorting of early endocytic vesicles. *Am J Physiol Gastrointest Liver Physiol*. 2014; 306:G412–24.  
<https://doi.org/10.1152/ajpgi.00118.2013>  
PMID:24407591
  28. She ZY, Pan MY, Tan FQ, Yang WX. Minus end-directed kinesin-14 KIFC1 regulates the positioning and architecture of the Golgi apparatus. *Oncotarget*. 2017; 8:36469–83.  
<https://doi.org/10.18632/oncotarget.16863>  
PMID:28430595
  29. Cross RA, McAinsh A. Prime movers: the mechanochemistry of mitotic kinesins. *Nat Rev Mol Cell Biol*. 2014; 15:257–71.  
<https://doi.org/10.1038/nrm3768> PMID:24651543
  30. She ZY, Yang WX. Molecular mechanisms of kinesin-14 motors in spindle assembly and chromosome segregation. *J Cell Sci*. 2017; 130:2097–110.  
<https://doi.org/10.1242/jcs.200261> PMID:28668932
  31. Fu X, Zhu Y, Zheng B, Zou Y, Wang C, Wu P, Wang J, Chen H, Du P, Liang B, Fang L. KIFC1, a novel potential prognostic factor and therapeutic target in hepatocellular carcinoma. *Int J Oncol*. 2018; 52:1912–22.



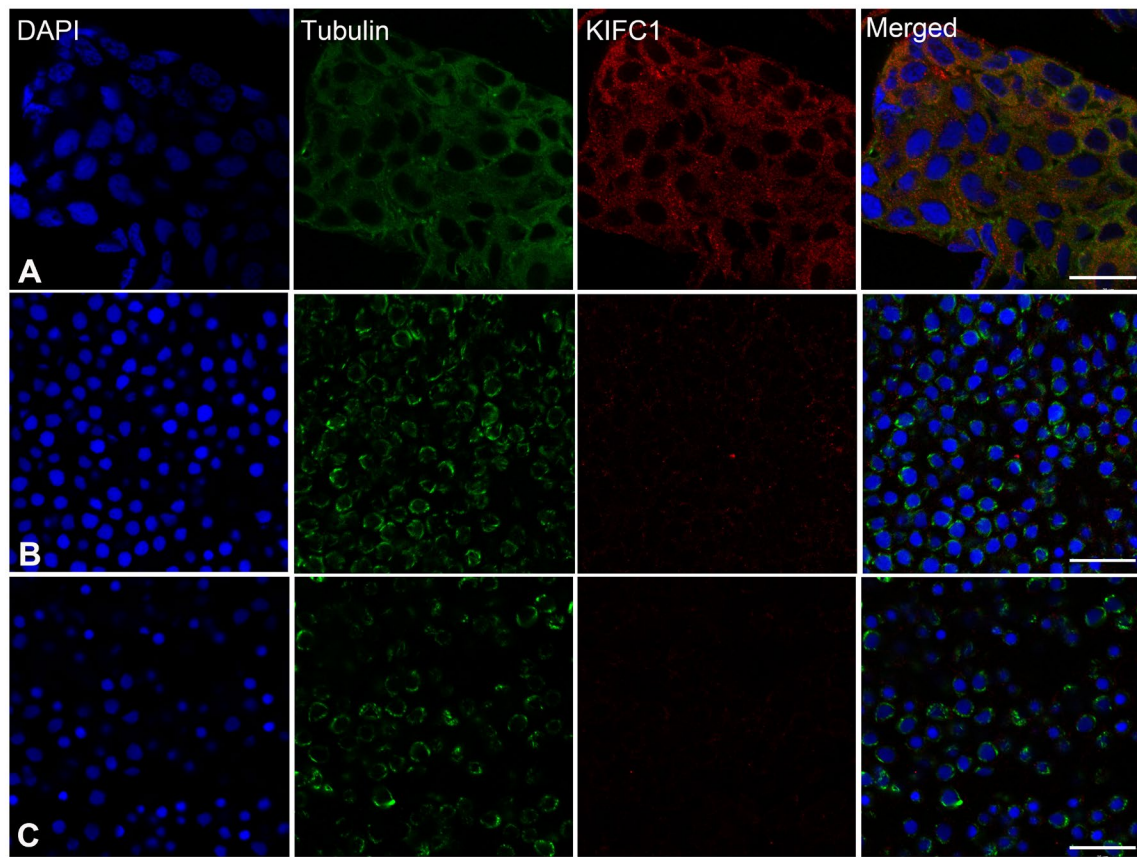
- <https://doi.org/10.3892/ijo.2018.4348>  
PMID:[29620256](https://pubmed.ncbi.nlm.nih.gov/29620256/)
32. Wang W, Zhu JQ, Yang WX. Molecular cloning and characterization of KIFC1-like kinesin gene (*ot-kifc1*) from *Octopus tankahkeei*. *Comp Biochem Physiol B Biochem Mol Biol*. 2010; 156:174–82.  
<https://doi.org/10.1016/j.cbpb.2010.03.004>  
PMID:[20304088](https://pubmed.ncbi.nlm.nih.gov/20304088/)
33. Ma DD, Pan MY, Hou CC, Tan FQ, Yang WX. KIFC1 and myosin Va: two motors for acrosomal biogenesis and nuclear shaping during spermiogenesis of *Portunus trituberculatus*. *Cell Tissue Res*. 2017; 369:625–40.  
<https://doi.org/10.1007/s00441-017-2638-4>  
PMID:[28639134](https://pubmed.ncbi.nlm.nih.gov/28639134/)
34. Hao SL, Zhang LY, Ping J, Wu XW, Hu JR, Zhang YP. Molecular cloning and putative functions of KIFC1 for acrosome formation and nuclear reshaping during spermiogenesis in schlegel's japanese gecko *Gekko japonicus*. *Asian Herpetol Res*. 2019.  
<https://doi.org/10.16373/j.cnki.ahr.180080>
35. Gao XM, Mu DL, Hou CC, Zhu JQ, Jin S, Wang CL. Expression and putative functions of KIFC1 for nuclear reshaping and midpiece formation during spermiogenesis of *Phascolosoma esculenta*. *Gene*. 2019; 683:169–83.  
<https://doi.org/10.1016/j.gene.2018.10.021>  
PMID:[30316921](https://pubmed.ncbi.nlm.nih.gov/30316921/)
36. Tsoi KH, Ma KY, Wu HT, Fennessy ST, Chu KH, Chan TY. Verification of the cryptic species *Penaeus pulchricaudatus* in the commercially important kuruma shrimp *P. japonicus* (Decapoda : Penaeidae) using molecular taxonomy. *Invertebr Syst*. 2014; 28:476–90.  
<https://doi.org/10.1071/IS14001>.
37. Yu K, Hou L, Zhu JQ, Ying XP, Yang WX. KIFC1 participates in acrosomal biogenesis, with discussion of its importance for the perforatorium in the Chinese mitten crab *Eriocheir sinensis*. *Cell Tissue Res*. 2009; 337:113–23.  
<https://doi.org/10.1007/s00441-009-0800-3>  
PMID:[19484267](https://pubmed.ncbi.nlm.nih.gov/19484267/)
38. Li Z, Pan CY, Zheng BH, Xiang L, Yang WX. Immunocytochemical studies of the acroframosome during spermiogenesis of the caridean shrimp *Macrobrachium nipponense* (Crustacea, Natantia). *Invertebr Reprod Dev*. 2010; 54:121–31.  
<https://doi.org/10.1080/07924259.2010.9652324>
39. Zhang Y, Sperry AO. Comparative analysis of two C-terminal kinesin motor proteins: KIFC1 and KIFC5A. *Cell Motil Cytoskeleton*. 2004; 58:213–30.  
<https://doi.org/10.1002/cm.20008>  
PMID:[15236353](https://pubmed.ncbi.nlm.nih.gov/15236353/)
40. Segbert C, Barkus R, Powers J, Strome S, Saxton WM, Bossinger O. KLP-18, a Klp2 kinesin, is required for assembly of acentrosomal meiotic spindles in *Caenorhabditis elegans*. *Mol Biol Cell*. 2003; 14:4458–69.  
<https://doi.org/10.1091/mbc.e03-05-0283>  
PMID:[12937278](https://pubmed.ncbi.nlm.nih.gov/12937278/)
41. Cai S, Weaver LN, Ems-McClung SC, Walczak CE. Kinesin-14 family proteins HSET/XCTK2 control spindle length by cross-linking and sliding microtubules. *Mol Biol Cell*. 2009; 20:1348–59.  
<https://doi.org/10.1091/mbc.e08-09-0971>  
PMID:[19116309](https://pubmed.ncbi.nlm.nih.gov/19116309/)
42. Fink G, Hajdo L, Skowronek KJ, Reuther C, Kasprzak AA, Diez S. The mitotic kinesin-14 Ncd drives directional microtubule-microtubule sliding. *Nat Cell Biol*. 2009; 11:717–23.  
<https://doi.org/10.1038/ncb1877> PMID:[19430467](https://pubmed.ncbi.nlm.nih.gov/19430467/)
43. Vicente JJ, Wordeman L. The quantification and regulation of microtubule dynamics in the mitotic spindle. *Curr Opin Cell Biol*. 2019; 60:36–43.  
<https://doi.org/10.1016/j.ceb.2019.03.017>  
PMID:[31108428](https://pubmed.ncbi.nlm.nih.gov/31108428/)
44. Lecland N, Lüders J. The dynamics of microtubule minus ends in the human mitotic spindle. *Nat Cell Biol*. 2014; 16:770–78.  
<https://doi.org/10.1038/ncb2996> PMID:[24976384](https://pubmed.ncbi.nlm.nih.gov/24976384/)
45. Kim N, Song K. KIFC1 is essential for bipolar spindle formation and genomic stability in the primary human fibroblast IMR-90 cell. *Cell Struct Funct*. 2013; 38:21–30.  
<https://doi.org/10.1247/csf.12014> PMID:[23318213](https://pubmed.ncbi.nlm.nih.gov/23318213/)
46. Choe MH, Kim J, Ahn J, Hwang SG, Oh JS, Kim JS. Centrosome Clustering Is a Tumor-selective Target for the Improvement of Radiotherapy in Breast Cancer Cells. *Anticancer Res*. 2018; 38:3393–400.  
<https://doi.org/10.21873/anticancer.12606>  
PMID:[29848688](https://pubmed.ncbi.nlm.nih.gov/29848688/)
47. Wei YL, Yang WX. Kinesin-14 motor protein KIFC1 participates in DNA synthesis and chromatin maintenance. *Cell Death Dis*. 2019; 10:402.  
<https://doi.org/10.1038/s41419-019-1619-9>  
PMID:[31127080](https://pubmed.ncbi.nlm.nih.gov/31127080/)
48. Pannu V, Rida PC, Ogden A, Turaga RC, Donthamsetty S, Bowen NJ, Rudd K, Gupta MV, Reid MD, Cantuaria G, Walczak CE, Aneja R. HSET overexpression fuels tumor progression via centrosome clustering-independent mechanisms in breast cancer patients. *Oncotarget*. 2015; 6:6076–91.  
<https://doi.org/10.18632/oncotarget.3475>  
PMID:[25788277](https://pubmed.ncbi.nlm.nih.gov/25788277/)
49. Sekino Y, Oue N, Koike Y, Shigematsu Y, Sakamoto N, Sentani K, Teishima J, Shiota M, Matsubara A, Yasui W.

- KIFC1 Inhibitor CW069 Induces Apoptosis and Reverses Resistance to Docetaxel in Prostate Cancer. *J Clin Med*. 2019; 8:E225.  
<https://doi.org/10.3390/jcm8020225> PMID:[30744126](https://pubmed.ncbi.nlm.nih.gov/30744126/)
50. De S, Cipriano R, Jackson MW, Stark GR. Overexpression of kinesins mediates docetaxel resistance in breast cancer cells. *Cancer Res*. 2009; 69:8035–42.  
<https://doi.org/10.1158/0008-5472.CAN-09-1224> PMID:[19789344](https://pubmed.ncbi.nlm.nih.gov/19789344/)
51. Zhang C, Chen X, Chen X, Wang X, Ji A, Jiang L, Sang F, Li F. miR-135a acts as a tumor suppressor in gastric cancer in part by targeting KIFC1. *Onco Targets Ther*. 2016; 9:3555–63.  
<https://doi.org/10.2147/ott.s105736> PMID:[27366092](https://pubmed.ncbi.nlm.nih.gov/27366092/)
52. Dumont J, Desai A. Acentrosomal spindle assembly and chromosome segregation during oocyte meiosis. *Trends Cell Biol*. 2012; 22:241–49.  
<https://doi.org/10.1016/j.tcb.2012.02.007> PMID:[22480579](https://pubmed.ncbi.nlm.nih.gov/22480579/)
53. Endow SA, Komma DJ. Assembly and dynamics of an anastral:astral spindle: the meiosis II spindle of *Drosophila* oocytes. *J Cell Sci*. 1998; 111:2487–95.  
<https://doi.org/10.1083/jcb.137.6.1321> PMID:[9701548](https://pubmed.ncbi.nlm.nih.gov/9701548/)
54. Park HW, Ma Z, Zhu H, Jiang S, Robinson RC, Endow SA. Structural basis of small molecule ATPase inhibition of a human mitotic kinesin motor protein. *Sci Rep*. 2017; 7:15121.  
<https://doi.org/10.1038/s41598-017-14754-6> PMID:[29123223](https://pubmed.ncbi.nlm.nih.gov/29123223/)
55. Ma DD, Bi L, Yang WX. KIFC1 participates in acrosome formation and nuclear shaping and is essential for spermiogenesis of red crayfish *Procambarus clarkii*. *Oncotarget*. 2017; 8:36082–98.  
<https://doi.org/10.18632/oncotarget.16429> PMID:[28415605](https://pubmed.ncbi.nlm.nih.gov/28415605/)
56. Yang WX, Jefferson H, Sperry AO. The molecular motor KIFC1 associates with a complex containing nucleoporin NUP62 that is regulated during development and by the small GTPase RAN. *Biol Reprod*. 2006; 74:684–90.  
<https://doi.org/10.1095/biolreprod.105.049312> PMID:[16371587](https://pubmed.ncbi.nlm.nih.gov/16371587/)
57. Wang W, Zhu JQ, Yu HM, Tan FQ, Yang WX. KIFC1-like motor protein associates with the cephalopod manchette and participates in sperm nuclear morphogenesis in *Octopus tankahkeei*. *PLoS One*. 2010; 5:e15616.  
<https://doi.org/10.1371/journal.pone.0015616> PMID:[21187923](https://pubmed.ncbi.nlm.nih.gov/21187923/)
58. Wang DH, Yang WX. Molecular cloning and characterization of KIFC1-like kinesin gene (es-KIFC1) in the testis of the Chinese mitten crab *Eriocheir sinensis*. *Comp Biochem Physiol A Mol Integr Physiol*. 2010; 157:123–31.  
<https://doi.org/10.1016/j.cbpa.2010.05.015> PMID:[20554056](https://pubmed.ncbi.nlm.nih.gov/20554056/)
59. Hou CC, Yang WX. Acroframosome-dependent KIFC1 facilitates acrosome formation during spermatogenesis in the caridean shrimp *Exopalaemon modestus*. *PLoS One*. 2013; 8:e76065.  
<https://doi.org/10.1371/journal.pone.0076065> PMID:[24098763](https://pubmed.ncbi.nlm.nih.gov/24098763/)
60. Hu JR, Liu M, Wang DH, Hu YJ, Tan FQ, Yang WX. Molecular characterization and expression analysis of a KIFC1-like kinesin gene in the testis of *Eumeces chinensis*. *Mol Biol Rep*. 2013; 40:6645–55.  
<https://doi.org/10.1007/s11033-013-2779-9> PMID:[24078165](https://pubmed.ncbi.nlm.nih.gov/24078165/)
61. Zhang DD, Gao XM, Zhao YQ, Hou CC, Zhu JQ. The C-terminal kinesin motor KIFC1 may participate in nuclear reshaping and flagellum formation during spermiogenesis of *Larimichthys crocea*. *Fish Physiol Biochem*. 2017; 43:1351–71.  
<https://doi.org/10.1007/s10695-017-0377-9> PMID:[28534180](https://pubmed.ncbi.nlm.nih.gov/28534180/)

## SUPPLEMENTARY MATERIALS



**Supplementary Figure 1. Immunofluorescent localization of KIFC1 and tubulin during spermatogenesis in the control group of *P. japonicus* testis.** (A) Spermatogonia and spermatocyte. No KIFC1 and microtubule signal was found in both spermatogonia (white arrow) and spermatocyte (yellow arrow). (B) Early spermatid and late spermatid. No KIFC1 and microtubule signal was found in both early spermatid (white arrow) and late spermatid (yellow arrow). Blue: DAPI, Green: tubulin, Red: KIFC1. Scale bar= 20 $\mu$ m.



**Supplementary Figure 2. Effects of the control dsRNA (dsEGFP) injected group on the expression and distribution of the microtubules in the testis, vas deferens and spermatophore.** (A) KIFC1 and microtubules in the testis. (B) KIFC1 and microtubules in vas deferens. (C) KIFC1 and microtubules in spermatophore. In the control dsRNA (dsEGFP) injected group, the expression and distribution of KIFC1 and microtubules are normal. Blue: DAPI, Green: tubulin, Red: KIFC1. Scale bar = 20 $\mu$ m.